SF Journal of Environmental and Earth Science

Effect by Seasons on Backscattering Intensity of ALOS-2 PALSAR-2 Data (L-band) to Retrieval Forest Biomass in Tropical Region

Luong VN*, Hieu VN, Tu TT, Thanh KTP, Tuan AP and Chi KT

Space Technology Institute, Vietnam Academy of Science and Technology, Cau Giay, Hanoi, Vietnam

Abstract

In this research we used the L-band radar from ALOS-2 PALSAR-2 and field work data for evaluation of effects by the season to retrieval forest biomass in tropical region. The effect of seasonality and HH, HV polarizations of the SAR data on the biomass was analyzed. The dry season HV polarization could explain 61% of the biomass in this study region. The dry season HV backscattering intensity was highly sensitive to the biomass compared to the rainy season backscattering intensity. The SAR data acquired in rainy season with humid and wet canopies were not very sensitive to the in situ biomass. The strong dependence of the biomass estimates with the season of SAR data acquisition confirmed that the choice of right season SAR data is very important for improving the satellite based estimates of the biomass. We expect that the results obtained in this research will contribute to monitoring of forest biomass and quality forest in Vietnam as well as tropical countries.

Keywords: L-band SAR; ALOS-2 PALSAR-2; HH; HV; Backscattering intensity; Biomass; Tropical forest and Season

Introduction

The role of forests to mitigate climate change has been strongly recognized again in the Paris Agreement, as "key components of landmark climate deal agreed as well as an instrument to contribute to reducing emissions and enhancing carbon sinks" [1]. The information of forest biomass is essential for increasing understanding of the terrestrial carbon cycle and judicial management of forest resources. Forests sequestrate atmospheric carbon dioxide in the form of biomass during photosynthesis [2-4]. Therefore, forest biomass has an important role in the global carbon cycle [5-7]. When forests are destroyed, more carbon is added to the atmosphere which accelerates climate change. Accurate monitoring of forest biomass and CO_2 sequestration rates are immensely important for increasing understanding of global carbon cycles, improving climate change forecasting models, and climate change mitigation and adaptation strategies [3,7-11]. Global monitoring of forest carbon is also urgently needed for the United Nation's program on Reducing Emissions from Deforestation and Degradation (REDD+), a financial payment mechanism for environmental services [11,12]. However, estimating biomass from satellite data is challenging due to the diverse nature of forests and tropical forests [7,10,13-15].

Satellite remote sensing technology has many advantages for biomass estimates over traditional field survey based methods, particularly at larger scales. Therefore, it has been used by many researchers for biomass estimates [7,14,16]. Satellite based estimation of biomass is based on optical, radar, and more recently lidar techniques. Limitations on optical data based biomass estimates have been reported by researchers such as saturation over large biomass regions, very low correlation, and difficulties in detecting vertical structure [7,9,15,17-21].

Lidar sensors have performed excellent estimates even in forests with high biomass and woody volumes by directly measuring the structure of the forest, i.e., canopy height and vertical distribution [13,18]. However, large scale application of lidar data is not economically feasible at present [7,14,20].

Radar remote sensing from satellites has high potential for biomass estimates at large scale because of its penetrability through clouds, applicability with night time, coverage at large scale, availability of seasonal data, and lower saturation in dense forests [7,15,22-30]. The long-wavelength SAR satellite is expected to have much promise for estimates of forest biomass [3,26,27,31].

OPEN ACCESS

***Correspondence:**
Luong Viet Nguyen, Space Technology Institute, Vietnam Academy of Science and Technology, Cau Giay, Hanoi, Vietnam.
E-mail: *nvluong@sti.vast.vn*

Received Date: *26 Jun 2020*
Accepted Date: *07 Sep 2020*
Published Date: *10 Sep 2020*

Citation: *Luong VN, Hieu VN, Tu TT, Thanh KTP, Tuan AP, Chi KT. Effect by Seasons on Backscattering Intensity of ALOS-2 PALSAR-2 Data (L-band) to Retrieval Forest Biomass in Tropical Region. SF J Environ Earth Sci. 2020; 3(2): 1041.*

ISSN 2643-8070

The backscattering intensity of L-band and P-band SAR data have demonstrated sensitivity to structure, cover, volume, and biomass of the forests penetrating into the branches and stems of trees [24,32-35]. A number of previous studies have shown an impressive relationship between the SAR data and biomass [23,35-42]. On the other hand, several researchers have reported saturation problems with the L-band SAR backscattering over high biomass regions. The major techniques for SAR based estimates of biomass attempted by a number of researchers so far are regression modelling [36,43-45], dual-wavelength SAR interferometry [34]; image texture analysis [46]; interferometric water cloud model, random volume over ground model, water cloud model [47], combination of forest structure and radiative transfer models [28], electromagnetic modelling [48], multivariate relevance vector regression [49]. SAR data have been used for estimating biomass at different scales from local to regional/country level: pine plantation in Southwest Alabama [23], Mount Sharsta region of Northern California [50], plantation forest of the Landes forest in southwestern France [36], Brazilian Amazon [39], Nuuksio Natural Park in Southern Finland, Queensland in Australia [51], Mozambique in Zambézia province [45], Cambodia [52], and Cameroon [48].

The Advanced Land Observing Satellite-2 [53], a Japanese satellite launched in 2014, which operates in L-band radar and collects very high spatial resolution. Currently, satellite image data from ALOS-2 is available and meets the global supply capability to many different applications.

The objective of this study was to assess the effects of seasons in the tropics on the quality of the ALOS-2 PALSAR-2 (L-band) satellite imagery.

Study Area and Data

Study area

Yok Don National Park (YDNP) is located in Dak Lac and Dak Nong provinces, Central Highlands of Vietnam. Currently, this park is the largest national park in Vietnam. This park was chosen for this study because several reasons bellow: (i) It is located in the tropical forest with characteristics of the typical structure in Vietnam; (ii) This park is the largest national park in Vietnam; (iii) It is located on relatively flat ground, average slope from 7o - 10o, thereby minimizing the effect of topography on this study; (iv) The road network around and inside the study area is not too difficult to transport, and perform fieldwork.

Yok Don National Park has the geographic coordinates between: From 12o45'-13o10' North latitude; From 107o29'30"-107o48'30" East longitude. The local map of the YDNP is shown in Figure 1.

Topography: The whole area is divided into two main geographical terrain forms: fairly smooth peneplain, and being lower towards the Mekong River. The other terrain form, low hills, and mountains is lying along the north riverbank. The topography of this park contains relatively plain topography and is located at an altitude of 200-300 m above sea level. Most of the terrain with an average slope from 7o-10o [54]. This terrain form is a good condition for the implementation of this study.

Climate: This region is a tropical monsoon that has a well-defined a distinct dry and rainy season. The rainy season concentrates between May to November. The average rainfall obviously changes among months of the rainy season and the dry season. It is very low in the dry season from October to April; the average value is less than 50 mm. In contrast, it is very high from April to August and then quickly decreases in September and October at the end of the rainy season. The average annual rainfall about 1,530 mm, while the average annual evaporation is 1,470 mm, and the mean monthly temperature is around 25°C [54].

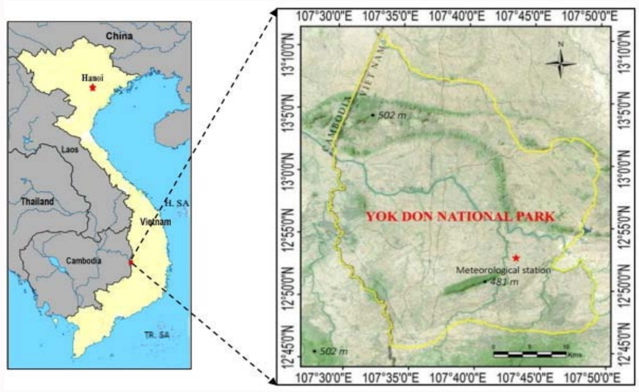

Figure 1: Location map of the study area displaying the boundary of Yok Don National Park (yellow polygon) in Central Highlands region, Vietnam.

Compared to rainfall and humidity, the monthly change of air temperature is very high. April and May are months whose average air temperature is highest, about 27°C, while the average temperature in December and January is lowest, about 14°C.

Biodiversity: This park is very rich in biodiversity where 854 species, belong to 478 vascular plant species and 129 families of 4 phyla of vascular plants have been recorded. This park has two major types of forest: deciduous broadleaf forest and evergreen broadleaf forest. The dominant tree species in the deciduous broadleaf forest are *Dipterocarpus tuberculatus, Dipterocarpus obtusifolius, Terminalia tomentosa*, and *Shorea obtuse*. The evergreen broadleaf forest mainly comprises of *Michelia mediocris, Cinamomum iners, Syzygium zeylanicum, Syzygium wightianum, Garruga pierrei, Gonocaryum lobbianum, Schima superba, Camellia assamica*, and *Lithocarpus fenestratus*. This park has 21 tree species in the list of the Red Data Book of Vietnam [54]. A total of 89 species of mammals, 250 species of birds, 48 species of reptiles, 16 species of amphibians, 31 species of fish, and 437 species of butterflies were recorded. This park is one of the most important protected areas and provides a suitable habitat for conservation of globally endangered species in Southeast Asia such as wild elephants, wild cow, deer and a lot of birds such as peacocks and several species of birds of prey and large water birds.

Satellite and processing data (ALOS-2 PALSAR-2)

In this study, we used the Advanced Land Observing Satellite-2 Synthetic Aperture Radar (ALOS-2 SAR), provided by Japan Aerospace Exploration Agency (JAXA), a Japanese satellite launched in 2014, which operates in L-band radar and collects very high spatial resolution data. ALOS-2 SAR data with version 2.1, which has 6.25 m pixel resolution was selected from February 2015 (dry season) and October 2014 (rainy season). The Digital Number (DN) values of the SAR images in both the HH and HV polarizations were calibrated by calculating the backscattering intensity using the Equation (1) [53].

$$\sigma^o = 10 x \log_{10} (DN^2) + CF \quad \ldots\ldots\ldots\ldots\ldots\ldots (1)$$

In Equation (1), the σ^o is the sigma-naught backscattering intensity in the units of decibels (dB), and CF is the Calibration

Table 1: The ALOS-2 PALSAR-2 data used in this research.

No.	Obs. date	Scene ID	Polar.	Obs. angle	Seasons
1	5 Oct. 2014	ALOS2019900240-141005-FBDR2.1GUA	HH, HV	32.9°	Rainy
2	5 Oct. 2014	ALOS2019900250-141005-FBDR2.1GUA	HH, HV	32.9°	Rainy
3	22 Feb. 2015	ALOS2040600240-150222-FBDR2.1GUA	HH, HV	32.9°	Dry
4	22 Feb. 2015	ALOS2040600250-150222-FBDR2.1GUA	HH, HV	32.9°	Dry

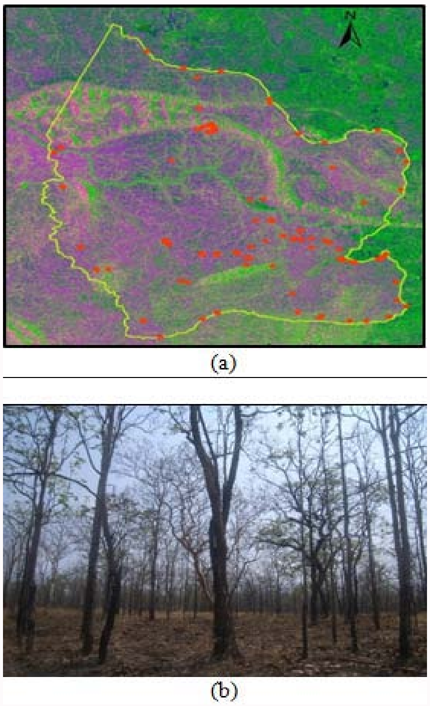

Figure 2: (**a**) The distribution of the location of sample plots established during field survey over the dry season RGB color composite images, and (**b**) Forest in rainy season.

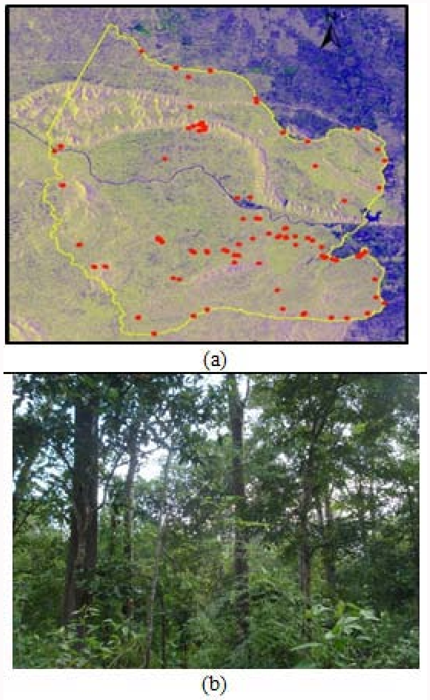

Figure 3: (**a**) The distribution of the location of sample plots established during field survey over the rainy season RGB color composite images: (**b**) Forest in rainy season.

Factor which is currently set as -83 [53].

The details on the ALOS-2 SAR images used in this research are described in Table 1. Both dry and rainy season SAR images were used, acquired with the same off-nadir angle (32.9°) in descending modes in order to avoid bias related to observation angles.

Methodology

Field worked

The *in situ* measurements were conducted by establishing the sample plots according to the inventory guideline available for the Central Highlands region [55,56]. All sample plots were established by meeting the criteria of representativeness of different forest types across the study areas. We carefully designed the sample plots in such a way that they were at least 100-m apart from trails, roads, streams, and rivers to avoid the signals from unwanted surface types for sensitivity analysis.

Each sample plot established during the forest inventory was (50 mx50 m) with an area of 0.25 ha. We measured the diameter at breast height (D) and total tree height (H) of all the trees larger than 5 cm diameter at breast height located inside the sample plots. The tree diameter and height were measured by using laser diameter and laser height instruments respectively. The central geo-location (latitude and longitude) of each sample plot was recorded by using GPS instruments.

The RGB color composite image was created by using the HH channel for red (R), HV channel for green (G), and the ratio HH/HV for blue (B). The distribution of sample plots used in this research are shown in Figure 2 and Figure 3 using RGB color composite of the SAR color composite images. Distinct variation between the rainy season and dry season RGB images in Yok Don National Park were observed as demonstrated in Figure 2 and Figure 3.

Estimation of forest biomass

We converted the individual tree biometry data: diameter at breast height (D) and total tree height (H) measured during the forest inventory into Above Ground Biomass (AGB) using the allometric equations. We used separate allometric equations for calculating the AGB of the deciduous and evergreen forests [56]. The allometric equations used for calculating the AGB of deciduous and evergreen forest types are given in Equation (2) and Equation (3) respectively.

$$AGB=0.14xD^{2.31} \quad \ldots\ldots\ldots\ldots\ldots\ldots(2)$$

$$AGB=0.098xexp(2.08xLn(D)+0.71xLn(H)+1.12xLn(WD)) \quad \ldots\ldots\ldots\ldots(3)$$

In Equation (2) and Equation (3), where:

AGB is the above ground biomass of a tree in kilograms (kg);

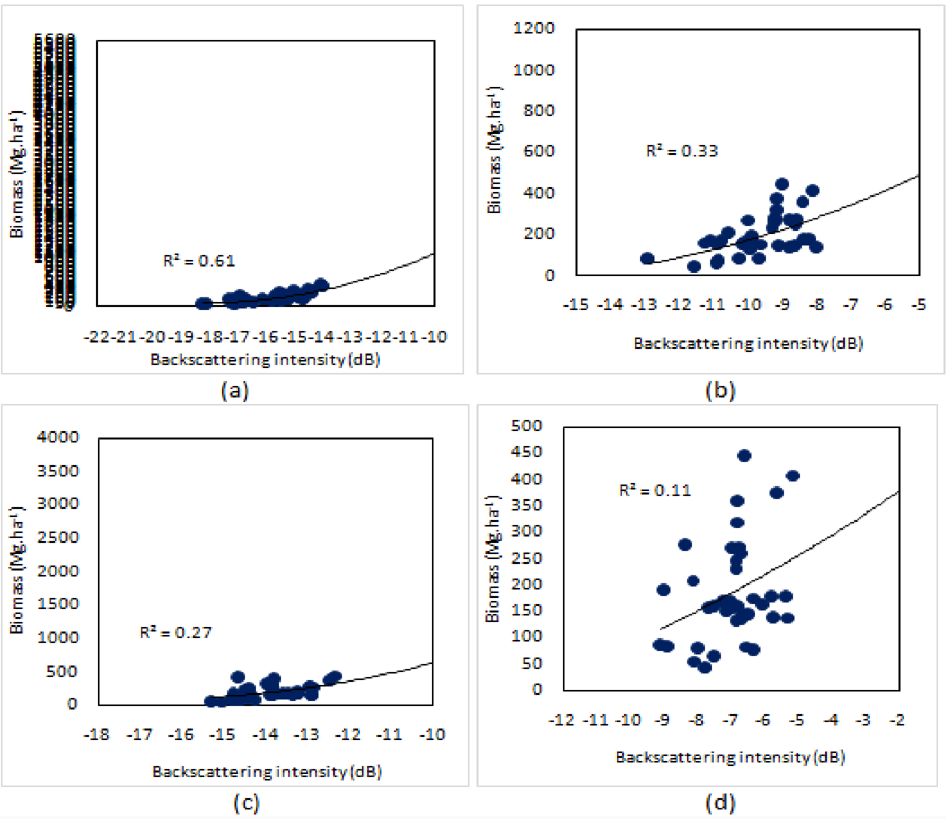

Figure 4: The relationship between the biomass, and backscattering intensity during dry season: (**a**) Biomass versus backscattering intensity (HV), (**b**) Biomass versus backscattering intensity (HH). The relationship between biomass and backscattering intensity during rainy season: (**c**) Biomass versus backscattering intensity (HV), (**d**) Biomass versus backscattering intensity (HH).

D is the diameter at breast height measured at 1.3 m above the ground level in meters (m);

H is the total height of tree in meters (m);

WD is the wood density of tree in tones dry matter per fresh cubic meters (ton/m^3).

Results and Discussions

Field survey results

The plot wise distribution of the forest structural variation is shown that: the sample plots represent larger variation of the diameter at breast height (8.14-48.74 cm), tree height (6.13-18.23 m), tree density (220-2800 trees.ha^{-1}) and biomass (42-450 Mg.ha^{-1}).

The polarizing difference of L-band SAR to the retrieval forest biomass

The sensitivity of biomass with the backscattering intensity of the HH and HV polarizations for the dry season was analyzed using the coefficient of determination (R^2) and Root Mean Square Error (RMSE). As shown in Figure 4a and Figure 4b, the HV polarization was highly related to both the biomass (R^2=0.61, RMSE=38.28 Mg.ha^{-1}); whereas the HH polarization did not show a significant relationship with the above ground biomass (R^2=0.33, RMSE=65.87 Mg.ha^{-1}).

The reason for the difference between the bellow correlation line and scattering above groups (In Figure 4) is because the different interaction between the signals obtained from the radar image is different between the high biomass forest and the low biomass forest.

The high sensitivity of the HV polarization towards biomass was found for both the dry and rainy season SAR data. This result highlighted the importance of HV polarization for the estimates of biomass.

The seasonal difference of L-band SAR to the retrieval forest biomass

The sensitivity of the ALOS-2 PALSAR-2 data (HV and HH polarizations) acquired during dry season and rainy season on biomass was analyzed. The relationship between biomass and dry season SAR data is shown in Figure 3a and Figure 3b; and the relationship between biomass and rainy season SAR data is shown in Figure 3c and Figure 3d. The dry season backscattering intensity of the HH and HV polarizations was highly sensitive to the biomass than the rainy season backscattering intensity. The higher relationship between the dry season HV polarization and biomass (R^2=0.61, RMSE=38.28 Mg.ha^{-1}) was obtained. However, the relationship between the rainy season HV polarization and biomass was relatively lower (R^2=0.27, RMSE=71.60 Mg.ha^{-1}) than the dry season. The relationship between rainy season HV polarization. This analysis suggests that dry season SAR data is more important for estimating the biomass than the rainy season data. The effect of seasonality for the SAR data was clearly observed in this research.

Validation result

We used 38 sample plots data were used to test the validity of the fitted linear regression models for the prediction of biomass. In Figure 5 shown, our model could explain 59% variation of the biomass (R^2=0.59, RMSE=40.28 Mg.ha^{-1}).

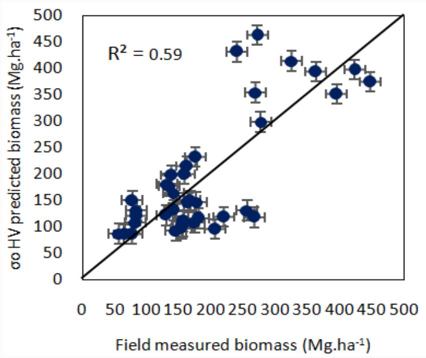

Figure 5: The validation of the SAR data based predicted results of above ground biomass. The 1:1 plot between the predicted and field data are shown.

Conclusions

In this research, the sensitivity of the biomass to the polarizations of ALOS-2 PALSAR-2 data (SAR data), and to the season of the acquisition of the SAR data were analyzed. The relationship between the ALOS-2PALSAR-2 based HV polarization backscattering intensity and field measured biomass since 59% variation in forest biomass could be explained by the HV polarization data. The resulting regression model is given in Equation 4 for biomass.

AGB (Mg.ha^{-1}) =16.028*(σ^oHV)^2+578.3*(σ^oHV)+5303 ....(4)

Where:

AGB is the above ground biomass in units of Mg.ha^{-1}.

The σ^o is the sigma-naught backscattering intensity of HV in the units of decibels (dB)

The saturation of the radar signal was clearly observed at high biomass level (250-300 Mg.ha^{-1} biomass). None of the biomass correlated with the rainy season HV polarization data as highly as the dry season HV polarization data. This study concluded and suggests that dry season SAR data is more important for estimating the biomass than the rainy season data. The effect of seasonality for the SAR data was clearly observed in this research. This results confirmed that the importance of SAR data mainly from the dry season.

Therefore, this research concluded that the choice of right season in which SAR data is acquired is a very important consideration for satellite based estimates of the biomass.

We expect that the results obtained in this research would be useful for promoting emission reduction programs in forestry sector, and achieving sustainable forest management goals in Vietnam as well as tropical countries.

Aknowlegements

The authors are grateful to theVT-CN.03/17-20 project under National Research on Space Science and Technology Program of Vietnam (2016-2020) for financial support to this research. We would like to thank JAXA for providing ALOS-2 PALSAR-2 data for this study in the frame work of ALOS Research program, PI No. 1172.

References

1. COP 21. 2015.

2. IPCC. Good Practice Guidance for Land Use, Land-Use Change and Forestry. 2003.

3. FAO. Global Terrestrial Observing System Rome. Assessment of the status of the development of the standards for the Terrestrial Essential Climate Variables, Rome. 2009.

4. Way AD, Pearcy WR. Sunflecks in trees and forests: from photosynthetic physiology to global change biology. Tree Physiol. 2012; 32: 1066-1081.

5. Brown S. Estimating biomass and biomass change of tropical forests: a primer. Food & Agriculture Org. 1997.

6. IPCC. Chapter 4: Forest Land. 2006 IPCC Guidelines for National Greenhouse Gas Inventories. 2006.

7. Gibbs HK, Brown S, Niles JO, Foley JA. Monitoring and estimating tropical forest carbon stocks: Making REDD a reality. Environ Res Lett. 2007.

8. FAO. Estimating Biomass and Biomass Change of Tropical Forests: a Primer. 1997.

9. GCOS. Systematic Observation Requirements for Satellite-based Products for Climate. Supplemental details to the satellite-based component of the Implementation Plan for the Global Observing System for Climate in Support of the UNFCCC. 2006.

10. FAO. Global Forest Resources Assessment 2010-Main Report. 2010.

11. Stone S, León CM. Climate Change & the Role of Forests A Community Manual. Conservation International. 2010.

12. UN-REDD Vietnam. Guidelines on Destructive Measurement for Forest Biomass Estimation in Vietnam-UN-REDD+. 2012.

13. Lefsky AM, Warren BC, Geoffrey GP, Harding JD. Lidar Remote Sensing for Ecosystem Studies. BioScience. 2002; 52: 19-30.

14. Lu D. The potential and challenge of remote sensing-based biomass estimation. Int J Rem Sens. 2006; 27: 1297-1328.

15. Sinha S, Jeganathan C, Sharma LK, Nathawat MS. A review of radar remote sensing for biomass estimation. Int J Environ Sci Technol. 2015; 12: 1779-1792.

16. Ghasemi N, Sahebi MR, Mohammadzadeh A. A review on biomass estimation methods using synthetic aperture radar data. Int J Geomat Geosci. 2011; 1: 776-788.

17. Ripple WJ, Wang S, Isaacson DL, Paine DP. A preliminary comparison of Landsat Thematic Mapper and SPOT-l HRV multispectral data for estimating coniferous forest volume. Int J Rem Sens. 1991; 12: 1971-1977.

18. Vincent MA, Saatchi SS. Comparison of remote sensing techniques for measuring carbon sequestration. JPL. 1999.

19. Gonzalez P, Asner GP, Battles JJ, Lefsky MA, Waring KM, Palace M. Forest carbon densities and uncertainties from Lidar, QuickBird, and field measurements in California. Rem Sens Environ. 2010; 114: 1561-1575.

20. Brewer KC, Monty J, Johnson A, Evans Fisk HD. Forest carbon monitoring: A review of selected remote sensing and carbon measurement tools for REDD+. 2011.

21. Pham TD, Xia J, Ha NT, Bui DT, Le NN, Tekeuchi W. A review of remote sensing approaches for monitoring blue carbon ecosystems: mangroves, seagrassesand salt marshes during 2010-2018. Sensors. 2019; 19: 1933.

22. Ulaby FT, Moore RK, Fung AK. Microwave remote sensing: active and passive. 1981.

23. Wu ST. Potential application of multipolarization SAR for pine-plantation biomass estimation. IEEE Trans. 1987; 25: 403-409.

24. Jensen JR. Remote sensing of the environment: An earth resource perspective. Pearson. 2007.

25. Kellndorfer J, Walker W, Pierce L, Dobson C, Fites JA, Hunsaker C, et al. Vegetation height estimation from shuttle radar topography mission and national elevation datasets. Rem Sens Environ. 2004; 93: 339-358.

26. Ramankutty N, Gibbs HK, Achard F, Defries R, Foley JA, Houghton RA.

Challenges to estimating carbon emissions from tropical deforestation. Global Change Biology. 2007; 13: 51-66.

27. Le Toan T, Quegan S, Davidson MWJ, Balzter H, Paillou P, Papathanassiou K, et al. The BIOMASS mission: Mapping global forest biomass to better understand the terrestrial carbon cycle. Rem Sens Environ. 2011; 115: 2850-2860.

28. Brolly M, Woodhouse IH. Long Wavelength SAR Backscatter Modelling Trends as a Consequence of the Emergent Properties of Tree Populations. Rem Sens. 2014; 6: 7081-7109.

29. Luong NV, Ryutaro T, Hoan TN, Ram CS, Tu TT, Son ML. Estimation of tropical forest structural characteristics using ALOS-2 SAR data. Advances in Remote Sensing. 2016; 5: 131-144.

30. Luong VN, Tu TT, Anh KL, Hong TX, Hoan NT, Thuy TLH. Biomass estimation and mapping of can GIO mangrove biosphere reserve in south of viet nam using ALOS-2 PALSAR-2 data. Appl Ecol Environ Res. 2019; 17: 15-31.

31. Pham TD, Le NN, Ha NT, Nguyen LV, Xia J, Yokoya N, et al. Estimating Mangrove Above-Ground Biomass Using Extreme Gradient Boosting Decision Trees Algorithm with Fused Sentinel-2 and ALOS-2 PALSAR-2 Data in Can Gio Biosphere Reserve, Vietnam. Rem Sens. 2020; 12: 777.

32. Sun G, Ranson JK, Kharuk lV. Radiometric slope correction for forest biomass estimation from SAR data in the Western Sayani Mountains, Siberia. Rem Sens Environ. 2002; 79: 279-287.

33. Balzter H. Forest mapping and monitoring with interferometric synthetic aperture radar (InSAR). Progress. 2001; 25: 159-177.

34. Balzter H, Rowland CS, Saich P. Forest canopy height and carbon estimation at Monks Wood National Nature Reserve, UK, using dual-wavelength SAR interferometry. Rem Sens Environ. 2007; 108: 224-239.

35. Mitchard ETA, Saatchi SS, Lewis LS, Feldpausch TR, Woodhouse IH, Sonke B, et al. Measuring biomass changes due to woody encroachment and deforestation/degradation in a forest-savanna boundary region of central Africa using multi-temporal L-band radar backscatter. Rem Sens Environ. 2011; 115: 2861-2873.

36. Le Toan T, Beaudoin A, Riom J, Guyon D. Relating forest biomass to SAR data. IEEE. 1992; 30: 403-411.

37. Dobson MC, Ulaby FT, Le Toan T, Beaudoin A, Kasischke ES, Christensen N. Dependence of radar backscatter on coniferous forest biomass. IEEE. 1992; 30: 412-415.

38. Ranson KJ, Sun G. Mapping biomass of a northern forest using multifrequency SAR data. IEEE. 1994; 32: 388-396.

39. Luckman A, Baker J, Kuplich MT, Yanasse FCC, Frery CA. A study of the relationship between radar backscatter and regenerating tropical forest biomass for spaceborne SAR instruments. Rem Sens Environ. 1997; 60: 1-13.

40. Santos JR, Lacruz MP, Araujo LS, Keil M. Savanna and tropical rainforest biomass estimation and spatialization using JERS-1 data. Int J Rem Sens. 2002; 23: 1217-1229.

41. Sandberg G, Ulander LM, Fransson JES, Holmgren J, Le Toan T. L- and P-band backscatter intensity for biomass retrieval in hemiboreal forest. Rem Sens Environ. 2011; 115: 2874-2886.

42. Peregon A, Yamagata Y. The use of ALOS/PALSAR backscatter to estimate above-ground forest biomass: A case study in Western Siberia. Rem Sens Environ. 2013; 137: 139-146.

43. Morel CA, Saatchi SS, Malhi Y, Berry JN, Banin L, Burslem D, et al. Estimating aboveground biomass in forest and oil palm plantation in Sabah, Malaysian Borneo using ALOS PALSAR data. Forest Ecology and Management. 2011; 262: 1786-1798.

44. Englhart S, Keuck V, Siegert F. Aboveground biomass retrieval in tropical forests - The potential of combined X- and L-band SAR data use. Rem Sens Environ. 2011; 115: 1260-1271.

45. Carreiras JMB, Melo JB, Vasconcelos MJ. Estimating the above-ground biomass in Miombo Savanna woodlands (Mozambique, East Africa) using L-band synthetic aperture radar data. Rem Sens. 2013; 5: 1524-1548.

46. Champion I, Dubois-Fernandez P, Guyon D, Cottrel M. Radar SAR images texture as a function of forest stand age. Int J Rem Sens. 2008; 29: 1795-1800.

47. Cartus O, Santoro M, Kellndorfer J. Mapping forest aboveground biomass in the Northeastern United States with ALOS PALSAR dual-polarization L-band. Rem Sens Environ. 2012; 124: 466-478.

48. Mermoz S, Réjou-Méchain M, Villard L, Le Toan T, Rossi V, Gourlet-Fleury S. Decrease of L-band SAR backscatter with biomass of dense forests. Rem Sens Environ. 2015; 159: 307-317.

49. Sharifi A, Amini J, Tateishi R. Estimation of forest biomass using multivariate relevance vector regression. Photogrammetric Engineering and Remote Sensing. 2015.

50. Richards J, Sun GQ, Simonett DS. L-band radar backscatter modeling of forest stands. IEEE. 1987; 25: 487-498.

51. Lucas R, Armston J, Fairfax R, Fensham R, Accad A, Carreiras J, et al. An evaluation of the ALOS PALSAR L-band backscatter-Above ground biomass relationship Queensland, Australia: Impacts of surface moisture condition and vegetation structure. IEEE Journal. 2010; 3: 576-593.

52. Avtar R, Suzuki R, Takeuchi W, Sawada H. PALSAR 50 m Mosaic Data Based National Level Biomass Estimation in Cambodia for Implementation of REDD+ Mechanism. PloS One. 2013; 8: e74807.

53. JAXA. ALOS-2/Calibration Result of JAXA standard products. 2014.

54. Nguyen TT. Modelling growth and yield of dipterocarp forests in Central Highlands of Vietnam. 2009.

55. Van Vo H, Van Tran H, Ngoc PB. Handbook for Vietnam forest inventory. 2006.

56. Tan Vu P, Viet NX, Trieu TD, Phung DT, Nguyen XG, Pham NT. PART B-6. Tree allometric equations in Evergreen broadleaf, Deciduous, and Bamboo forest in Central Highland region, Vietnam. UN-REDD Vietnam Programme. 2012.